Am J Transl Res 2021;13(9):10298-10314
www.ajtr.org /ISSN:1943-8141/AJTR0108984

Original Article

ITIH5 shows tumor suppressive properties in cervical cancer cells grown as multicellular tumor spheroids

Ann-Kathrin Daum[1,7], Jessica Dittmann[1], Lars Jansen[1], Sven Peters[2], Uta Dahmen[3], Julia I Heger[4], Felix Hoppe-Seyler[5], Alexandra Gille[1], Joachim H Clement[6], Ingo B Runnebaum[1], Matthias Dürst[1], Claudia Backsch[1]

[1]Department of Gynecology and Reproductive Medicine, Jena University Hospital, Friedrich-Schiller-University, Jena, Germany; [2]Department of Ophthalmology, Jena University Hospital, Friedrich-Schiller-University, Jena, Germany; [3]Experimental Transplantation Surgery, Department of General, Visceral and Vascular Surgery, Jena University Hospital, Friedrich-Schiller-University, Jena, Germany; [4]Placenta-Lab, Department of Obstetrics, Jena University Hospital, Friedrich-Schiller-University, Jena, Germany; [5]Molecular Therapy of Virus-Associated Cancers, German Cancer Research Center (DKFZ), Heidelberg, Germany; [6]Department of Hematology and Medical Oncology, Jena University Hospital, Friedrich-Schiller-University, Jena, Germany; [7]Current address: German Cancer Research Center (DKFZ), Division of Cancer Genome Research, Heidelberg, Germany

Received February 10, 2020; Accepted June 28, 2021; Epub September 15, 2021; Published September 30, 2021

Abstract: Cervical cancer (CC) arises from premalignant cervical intraepithelial neoplasia (CIN) induced by a persistent infection with human papillomaviruses. The multi-stepwise disease progression is driven by genetic and epigenetic alterations. Our previous studies demonstrated a clear downregulation of inter-α-trypsin-inhibitor-heavy chain 5 (*ITIH5*) at mRNA and protein levels in CC compared to CIN2/3 and normal cervical tissue. Initial *in vitro* functional analyses revealed a suppressive effect of ITIH5 on relevant mechanisms for cancer progression in conventional two dimensional (2D) cell culture model systems. Based on these studies, we aimed to investigate the functional relevance of ITIH5 in multicellular tumor spheroid (MCTS) models, which resemble *in vivo* tumors more closely. We successfully established CC cell line-derived MCTS using the hanging-drop technique. ITIH5 was ectopically overexpressed in HeLa and SiHa cells and its functional relevance was investigated under three dimensional (3D) culture conditions. We found that ITIH5 re-expression significantly suppressed tumor spheroid growth and spheroid invasiveness of both HeLa and SiHa spheroids. Immunohistochemical (IHC) analyses revealed a significant reduction in Ki-67 cell proliferation index and CAIX-positive areas indicative for hypoxia and acidification. Furthermore, we observed an increase in cPARP-positive cells suggesting a higher rate of apoptosis upon ITIH5 overexpression. An effect of ITIH5 expression on the susceptibility of cervical MCTS towards cytostatic drug treatment was not observed. Collectively, these data uncover pronounced anti-proliferative effects of ITIH5 under 3D cell culture conditions and provide further functional evidence that the downregulation of ITIH5 expression during cervical carcinogenesis could support cancer development.

Keywords: Cervical carcinogenesis, human papillomavirus, ITIH5, tumor suppressor gene, 3D cell culture

Introduction

Cervical cancer (CC) ranks the fourth leading cause of cancer-related mortality in females worldwide, accounting for 311,365 deaths in 2018 [1]. Approximately 80% of invasive CC represent squamous cell carcinomas (SSC), whereas adenocarcinomas (ADC) encompass 15% of the cases [2, 3]. These two distinct histological subtypes are preceded by non-invasive precancerous lesions, referred to as cervical intraepithelial neoplasia (CIN, graded I-III) and adenocarcinoma *in situ* (ACIS), respectively [4, 5].

A persistent infection with high-risk human papillomaviruses (hrHPV) is proven to be compulsory for the development of CC [6, 7]. Further (epi)genetic alterations of infected host cells, however, are indispensable for disease progression, since the sole infection is not sufficient for malignant transformation [8, 9]. In

order to identify putative tumor suppressor genes (TSGs) in previously localized chromosomal regions [10, 11], microarray expression analyses were employed. It could be demonstrated that inter-α-trypsin inhibitor heavy chain 5 (*ITIH5*) expression was significantly downregulated in CC compared to high-grade lesions (CIN3) [12]. A significant decrease of ITIH5 mRNA and protein expression in CC versus CIN2/3 and normal cervical tissue was further verified by quantitative real-time PCR (qPCR) and immunohistochemical analysis (IHC) [13]. Functional analyses using *in vitro* gain-of-function models demonstrated tumor suppressor properties including reduced proliferative and migratory capacities of ITIH5 in CC cell lines. Furthermore, loss of ITIH5 expression in microdissected CC tissue was associated with *ITIH5* promoter methylation, which could be restored by pharmacological DNA demethylation in CC cell lines [13].

ITIH5 is one of several members of inter-α-trypsin inhibitors, which belong to a family of serine protease inhibitors, consisting of one light chain (bikunin) and one or two homologues heavy chains (ITIH1-5) [14, 15]. ITIHs are known to bind covalently to hyaluronic acid (HA), a major macromolecule of the extracellular matrix (ECM), resulting in stabilization of the ECM, which in turn plays a decisive role in different physiological and pathological processes [16, 17]. There is strong evidence that altered ITIH expression is associated with tumorigenesis and metastasis [18, 19]. It could be shown that ITIH2-mediated ECM stabilization resulted in suppression of invasion [20], whereas ITIH1 and ITIH3 significantly reduced the number of metastases in a murine *in vivo* model [19]. Loss of *ITIH5* expression caused by an aberrant hypermethylation of the *ITIH5* promoter region was first described in breast cancer [21, 22]. To date, downregulation of ITIH5 expression is evident in several malignancies including acute myeloid leukemia (AML) [23], pancreatic ductal adenocarcinoma (PDAC) [24] and thyroid carcinomas [25]. Unfavorable patients' outcome and disease progression are further associated with loss of ITIH5 expression in tumors of bladder [26], colon [27] and lung [28]. Beyond that, *in vitro* studies of several cancer cell lines revealed inhibitory effects of ITIH5 re-expression on pathophysiological mechanisms crucial for progressive oncogenesis [13, 29, 30].

Previous studies already suggested a tumor suppressive function of ITIH5 in CC based on conventional 2D cell culture systems. Unlike monolayer cultures, the spatial arrangement within MCTS conserves morphological and functional differentiation as well as a histotypic organization of the tumor cells [31, 32]. However, there is no report showing the influence of ITIH5 on cervical tumor spheroid growth and other oncogenic properties. We therefore investigated the effects of ectopic ITIH5 re-expression on spheroid growth and invasion using two *in vitro* 3D cell culture models. Immunohistochemical analyses were applied to elucidate the impact of ITIH5 overexpression on cell proliferation, hypoxia and acidification well as apoptosis. In addition, the influence of ITIH5 on the susceptibility of cervical MCTS towards cytostatic drug treatment was examined.

Materials and methods

Cell lines

HPV18-positive HeLa (RRID: CVCL_0030) and HPV16-positive SiHa cells (RRID: CVCL_0032) were cultured in 25 cm^2 and 75 cm^2 flasks in Dulbecco's Modified Eagle's Medium (DMEM) supplemented with 10% fetal calf serum (FCS) (Sigma-Aldrich, Steinheim, Germany) and 100 U/ml penicillin and 100 µg/ml streptomycin (Life Technologies, Darmstadt, Germany). Flasks were maintained under standard conditions (5% CO_2, 37°C, 95% humidity). Both cell lines were authenticated by multiplex short tandem repeat analysis and the results of the PowerPlex 16 HS System (Promega, Madison, USA) were compared with the DSMZ database (http://www.dsmz.de).

Lentivirus-mediated gene transfer

Infectious lentiviral particles incorporating either pCDH empty vector or pCDH-ITIH5 were available from a previous study [13]. Approximately 24 h prior transduction, the two target cell lines, HeLa and SiHa, were seeded into 12-well plates and grown to 70-80% confluence. On the following day, growth medium was replaced by viral supernatants (1 ml/well) of empty-vector (mock) or ITIH5-expressing lentiviruses, previously mixed with 2 µg/ml polybrene (Sigma-Aldrich, Steinheim, Germany). Spinfection was performed at 1500 rpm for 45

min and the plates subsequently incubated at 37°C for 6 h. A second infection cycle was performed without polybrene, pursuant to the steps as described above. 48 h after the second infection cycle, cells were expanded into 25 cm^2 flasks followed by puromycin selection (Sigma-Aldrich, Steinheim, Germany) optimized for each cell line (SiHa 0.6 µg/ml; HeLa 0.5 µg/ml). Puromycin-containing medium was changed every other day for 7-9 days until non-transduced control cells (native) were dead (day 0 post-selection). Stable ITIH5 expression of transduced cells was investigated by both qPCR and immunocytochemistry 10 days post-selection.

RNA extraction, cDNA synthesis, and qPCR

Total RNA of HeLa and SiHa cells was isolated and purified using the NucleoSpin RNA Kit (Macherey-Nagel, Düren, Germany) in agreement with the manufacturer's protocol. Extracted RNA was converted into complementary DNA using oligo(dT) primer and SuperScript II reverse transcriptase (Life Technologies, Darmstadt, Germany). The FastStart SYBR Green PCR system (Roche, Mannheim, Germany) was used to determine *ITIH5* expression levels via qPCR on an ABI 7300 Sequence Detection System (Applied Biosystems, Darmstadt, Germany). See Table S1 for corresponding primer sequences. The PCR was performed according to the following steps: initial denaturation at 95°C for 10 min, 40 cycles: 15 sec 95°C, 20 sec 54°C, 40 sec 72°C, followed by melting curve analysis. Relative gene expression was calculated using the $\Delta\Delta C_t$-method [33]. The LinRegPCR program was applied for the determination of mean PCR efficiencies [34]. Normalization of *ITIH5* expression was conducted to the housekeeping gene actin beta (*ACTB*).

3D cell cultivation

MCTS were initiated in the presence of methylcellulose (MC) (Sigma-Aldrich, Steinheim, Germany). MC stock solution was prepared as described elsewhere [35]. Tumor spheroids were generated using the hanging-drop method (HD) according to a modified protocol of another study [36]. Briefly, cells were grown to 80% confluence. 20 µl drops containing 1,000 HeLa cells or 2,500 SiHa cells supplemented with 25% MC stock solution were pipetted onto the inner side of the lid of petri dishes. The bottom of the petri dish was filled with 5 ml DPBS to sustain a humid atmosphere. The lid was carefully turned upside down and placed on the dish. Thereby spheroid formation was initiated, which was considered as day 0. Spheroids formed within 4 days at 37°C and were transferred into single wells of non-tissue culture treated round-bottom 96-well plates (Greiner Bio-One, Kremsmünster, Austria) for further cultivation up to 12 days. Medium had to be changed every 3-4 days by a 50% medium replenishment.

Spheroid growth assay

HeLa and SiHa spheroids were generated and transferred into round-bottom 96-well plates as described above. Spheroid growth was assessed every other day up to day 12, starting at day 4 after spheroid initiation (considered as t0). For this purpose, phase-contrast images were captured at 50× magnification using an inverted microscope equipped with a digital camera. MCTS area (µm^2) was evaluated using the freehand selection tool of the image analysis software ImageJ (NIH, Bethesda, USA) [37].

Spheroid invasion assay

The invasive capability of tumor spheroids was investigated using a spheroid invasion assay, as described elsewhere [38]. Briefly, spheroids were generated and transferred into round-bottom 96-well plates as described above and cultivated in high glucose (4 g/l glucose) DMEM for 4 days. Half of the medium was replaced by Matrigel™ (Corning Incorporated, New York, USA) and allowed to solidify for 1 h at 37°C. 100 µl DMEM including 10% FCS was added on top of the gel (considered as t0). Images were taken from t0 and at intervals every other day up to day 10 post initiation. The invasive area (µm^2) was measured as the area covered by invading cells using ImageJ software (NIH, Bethesda, USA) [37].

Cell block preparation and immunocytochemistry

Cells grown as monolayers or 32 individual tumor spheroids were harvested at designated time points, pelleted and washed once with 10 ml DPBS. After resuspension in 100 µl DPBS containing Ca^{2+}/Mg^{2+}, 150 µl EDTA-Plasma

(Sigma-Aldrich, Steinheim, Germany) and 150 µl thrombin (1000 U/ml; Sigma-Aldrich, Steinheim, Germany) were added to the cells or spheroids and mixed gently. Coagulation was completed after 10 min incubation. Cell or spheroid clots were transferred into 5 ml Roti-Histofix (Roth, Karlsruhe, Germany) for overnight fixation, embedded in paraffin and trimmed in 3 µm-thick sections.

Hematoxylin-eosin staining and immunohistochemistry

Serial formalin-fixed paraffin-embedded (FFPE) cell and spheroid sections (3 µm) were dewaxed and rehydrated in xylene and a descending ethanol series, respectively. From each spheroid specimen, the first and last sections were stained with hematoxylin-eosin (HE) for assessment of spheroid morphology. Heat-induced epitope retrieval was performed for 20 min in pre-heated 10 mM citrate buffer (pH 6.0). Endogenous peroxidases were quenched by incubating the slides in 3% hydrogen peroxide (H_2O_2), followed by an overnight incubation with primary antibodies at 4°C. The following primary antibodies were applied: anti-ITIH5 (antibody was kindly provided by Dr. Kloten and Prof. Dr. Dahl, Institute of Pathology, Medical Faculty of the RWTH Aachen University, Aachen, Germany), anti-Ki67 (clone MIB-1; Dako, Hamburg, Germany), anti-CAIX (Abcam, Cambridge, UK), anti-cPARP (CST, Danvers, US). Cell block sections were stained with anti-ITIH5 only, while spheroid sections were stained with all above described antibodies. Secondary antibody staining and visualization of the reaction were performed using the Dako REAL™ EnVision™ Detection System (Peroxidase/DAB, Rabbit/Mouse; Dako, Hamburg, Germany). Cell nuclei were counterstained via incubation with hematoxylin. Cell block sections were inspected using an Axioplan 2 microscope and AxioVision Rel.4.8 software (Zeiss, Jena, Germany). Stained spheroid sections were scanned with high-resolution using a NanoZoomer 2.0-HT digital slide scanner (Hamamatsu Photonics, Hamamatsu, Japan). Quantitative analysis of digital IHC images stained for Ki-67, CAIX and cPARP was performed using ImageJ software (NIH, Bethesda, USA) [37] in combination with IHC Profiler, which includes two open source-macros for either nuclear or cytoplasmic IHC staining's, respectively [39]. In total, 3-4 sections of 8 individual spheroids were examined for each antibody stain.

Live/dead-assay using confocal laser scanning microscopy

For the treatment with two FDA-approved cytostatic drugs, cisplatin and paclitaxel [40], MCTS were generated and transferred to non-tissue culture treated round-bottom 96-well plates for further cultivation as described above. 8 days old spheroids were exposed to three drug concentrations of cisplatin (10 µM, 50 µM and 100 µM) and paclitaxel (100 nM, 1 µM, 10 µM) for 24 and 48 h, respectively. Treatment with 1% Triton X-100 served as a positive control. Cell viability within spheroids following drug exposure was assessed using the Live/Dead Viability/Cytotoxicity Kit (ThermoFisher Scientific, Massachusetts, USA) according to the manufacturer's instructions. Briefly, spheroids were transferred into glass-bottom 96 well-plates and washed with pre-warmed DPBS. Spheroids were stained with an ethidium homodimer-1 (EthD-1)-calcein AM mixture via incubation for 1 h at 4°C, followed by incubation for 30 min at 37°C. After a final washing procedure, the spheroid samples were imaged using an LSM 710 microscope (Zeiss, Jena, Germany) in combination with a titanium-sapphire laser. Scanning was performed with single excitation at 488 nm using spectral imaging, with 20×/0.4 detection optics and a 512×512-pixel resolution. The obtained emission profiles from each pixel of the microscopic image were separated by spectral unmixing using Zen-software (Zeiss, Jena, Germany). Separated channels representing either calcein AM or EthD-1 were quantified based on mean grey values using ImageJ (NIH, Bethesda, USA) [37] and resulting live/dead cell ratios were calculated.

Statistical analysis

For statistical analysis, GraphPad Prism 7 (GraphPad Software, San Diego, USA) was used. Two-way ANOVA followed by Tukey's multiple comparison test was applied to determine statistical significance of spheroid growth and invasion over time. One-way ANOVA followed by Tukey's multiple comparison test was used to analyze statistical significance of IHC staining positivity and live/dead cell ratios. Data were presented as mean ± standard deviation (SD).

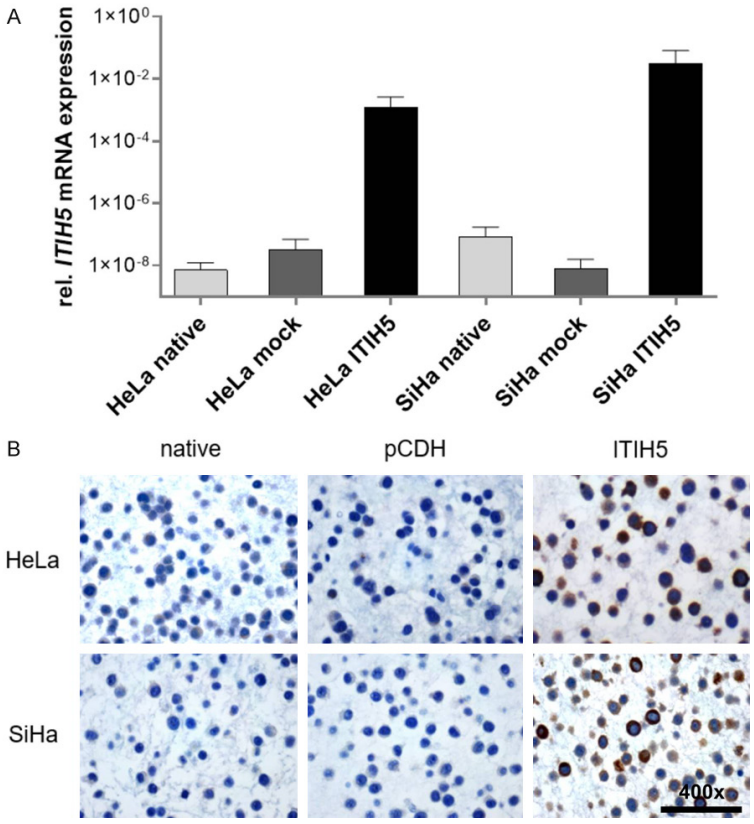

Figure 1. ITIH5 gain-of-function *in vitro* models show high *ITIH5* expression levels. Mock- and ITIH5-transduced HeLa and SiHa cells underwent puromycin selection and were harvested 10 days post-selection including a native, non-selected control. Characterization of ITIH5 expression was performed on mRNA and protein levels. A. Relative *ITIH5* mRNA expression of native, mock- and ITIH5-transduced cells was determined by qPCR. *ACTB* served as standard for normalizing relative *ITIH5* expression. Bars represent mean ± SD from biological duplicate samples in technical triplicates. B. Representative images of immunocytochemical analysis showing ITIH5 protein expression level in native and (mock-) transduced cells. Scale bar: 200 µm.

Differences were considered statistically significant if the two-sided *P*-values were equal or below 5% (≤0.05).

Results

Generation of ITIH5-overexpressing in vitro models

First *in vitro* analyses of CC cell lines overexpressing ITIH5 revealed tumor suppressive properties in a conventional 2D cell culture system [13]. In order to unravel the functional impact of ITIH5 silencing in a 3D environment, two CC cell lines (HeLa and SiHa) were transduced with *ITIH5*, followed by puromycin selection. Both cell lines exhibit only traces of endogenous *ITIH5* expression (**Figure 1**) and therefore serve as suitable model systems for *ITIH5* re-expression (gain-of-function) using lentivirus-mediated transduction of full-length *ITIH5* cDNA pCDH expression vector (ITIH5 clones) or the empty vector alone (mock clones). Successful overexpression of ITIH5 in transduced HeLa and SiHa cells and only marginal expression in native and mock-transduced cells was verified by qPCR (**Figure 1A**) as well as immunocytochemistry (**Figure 1B**) 10 days post-selection. A remarkable upregulation in mRNA and protein expression levels of ITIH5 was observed for both ITIH5-expressing *in vitro* cell culture models. By contrast, only traces of ITIH5 were detected in mock-transduced and native cells.

Reduced growth and invasiveness of HeLa and SiHa tumor spheroids after ITIH5 re-expression

Both *in vitro* models were used to characterize the effect of ITIH5 on functional tumor cell properties in a 3D culture system. The sustainability of proliferative capacity and high growth rates are one of the hallmarks of cancer cells [41]. Hence, MCTS growth of HeLa and SiHa spheroids derived from native, mock- and ITIH5-transduced cells was evaluated over time and relative spheroid growth rates were determined. It could be demonstrated that growth kinetics of HeLa (**Figure 2A**, left panel) and SiHa (**Figure 2A**, right panel) spheroids were slightly, but significantly retarded upon overexpression of ITIH5. In HeLa spheroids, ITIH5 re-expression reduced spheroid growth by 16.1% and 14.6%, respectively, in comparison to native and mock-transduced spheroids after 12 days of cultivation. Furthermore, SiHa spheroid growth rates were significantly decreased by 18.3% and 23.5%, respectively, upon ITIH5 overexpression as compared to spheroids derived from native and mock-transduced cells.

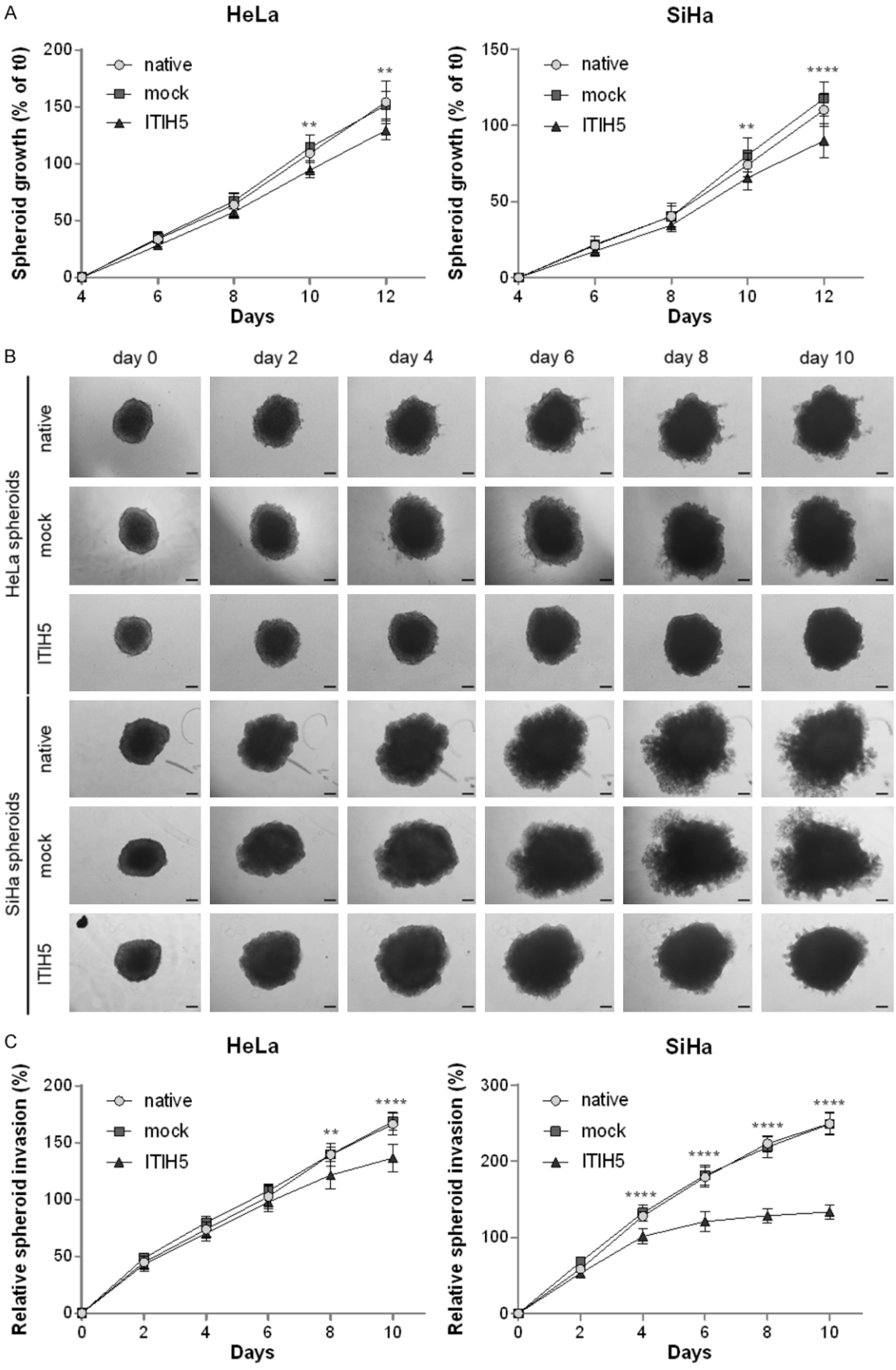
A
HeLa
SiHa
native
mock
ITIH5
Spheroid growth (% of t0)
Days
B
day 0
day 2
day 4
day 6
day 8
day 10
HeLa spheroids
SiHa spheroids
native
mock
ITIH5
C
HeLa
SiHa
Relative spheroid invasion (%)
Days

Figure 2. ITIH5 overexpression reduces cervical MCTS growth rates and invasiveness. A. Relative tumor spheroid growth rates of native, mock- and ITIH5-transduced HeLa and SiHa cells were determined by time course-measurements up to 8 days post-spheroid initiation. Spheroid area was determined every other day using phase-contrast imaging. Data were normalized to area values of day 4 (t0). Results are expressed in bars as mean ± 95% CI of 8 spheroids per condition (n = 3), $^{**}P < 0.01$, $^{****}P < 0.0001$ compared to the mock-control. B. Invasive capacity of tumor spheroids derived from HeLa and SiHa cells was evaluated over time using Matrigel-based invasion assay. Upper panel: Representative images of matrix-embedded HeLa spheroids at day 10 post-spheroid initiation used for quantification of relative invasion rates. Lower panel: Representative images of matrix-embedded SiHa spheroids 10 days post-spheroid initiation used for quantification of relative invasion rates. Scale bar: 50 µm. C. Relative spheroid invasion rates of native, mock- and ITIH5-transduced HeLa and SiHa spheroids was determined at different time points. Data were normalized to invasive area values of day 0 (t0). Bars represent mean ± 95% CI of 6 spheroids per condition (n = 3), $^{**}P < 0.01$, $^{****}P < 0.0001$ compared to the mock-control.

We next examined the invasive behavior of tumor cells, which is of high clinical significance and has a great prognostic value in terms of overall patient survival and therapy outcome [42]. Accordingly, MCTS were embedded into basement-membrane like matrix (Matrigel™) to investigate the invasiveness of spheroids derived from native, mock- and ITIH5-transduced HeLa and SiHa cells. HeLa spheroids of native and mock-transduced cells exhibit marginal invasive protrusions (**Figure 2B**, upper panel), whereas no invasive protrusions could be observed for HeLa spheroids upon ITIH5 overexpression (**Figure 2B**, lower panel). This was further illustrated by evaluating relative spheroid invasion rates. MCTS derived from ITIH5-overexpressing HeLa cells showed significantly decreased invasion rates (**Figure 2C**, left panel). The invasive capability decreased by 17.9% and 19.1%, respectively, as indicated by areas covered with invasive protrusions and compared to spheroids of native and mock-transduced HeLa cells on day 10. SiHa spheroids grown from native and mock-transduced cells exhibited clear branch-like invadopodia projecting into the surrounding matrix (**Figure 2B**, lower panel). In contrast, almost no protrusions were present when ITIH5 was re-expressed in SiHa spheroids. Relative invasion rates demonstrated additionally a dramatic reduction of the invasive capability of ITIH5-overexpessing SiHa spheroids (**Figure 2C**, right panel). The most distinct effect was detected on day 10, where the invasive areas of ITIH5-overexpressing SiHa spheroids were significantly decreased by 46.6% and 46.5%, respectively, compared to spheroids derived from native and mock-transduced cells.

Altogether, re-expression of ITIH5 leads to a significant decrease in spheroid growth over time and a pronounced suppression of tumor cell invasion in HeLa and SiHa spheroids, although to a different extent depending on the cell line.

ITIH5 promoted apoptosis while suppressed proliferation and hypoxia of CC spheroids in a cell type-dependent manner

To further characterize whether ITIH5 overexpression influences cervical MCTS morphologically and functionally, different histological staining protocols were applied. HE-staining of sectioned day 6 and day 12 HeLa (**Figure 3A**, **3B**) and SiHa (Figure S1A, S1B) spheroids revealed a dense morphology for both cell types and a for tumor spheroids typical layered structure with internal regions exhibiting signs of necrosis. The observed necrotic core regions were more pronounced for SiHa spheroids (day 6 and day 12) compared to spheroids derived from HeLa cells (day 12 only). However, no differences in spheroid morphology and internal necrotic areas were observed among spheroids from native, mock- and ITIH5-transduced HeLa and SiHa cells, respectively.

Verification of ITIH5 expression in 3D cultured HeLa and SiHa cells could be successfully demonstrated, as displayed by representative spheroid images in **Figures 3** and S1. Of note, ITIH5-positive cells were evidently located at the core region of HeLa spheroids on day 12, while ITIH5 expression was distributed throughout entire SiHa cell-derived spheroids. Nevertheless, a considerable overexpression of ITIH5 in HeLa and SiHa spheroids compared to spheroids of native and mock-transduced cells was detectable.

Antibody-based staining of protein targets was further applied to evaluate cell proliferation (Ki-67), hypoxia and acidification (CAIX) as well as apoptosis (cPARP) in cervical MCTS. Native and mock-transduced HeLa spheroids on day 6 and

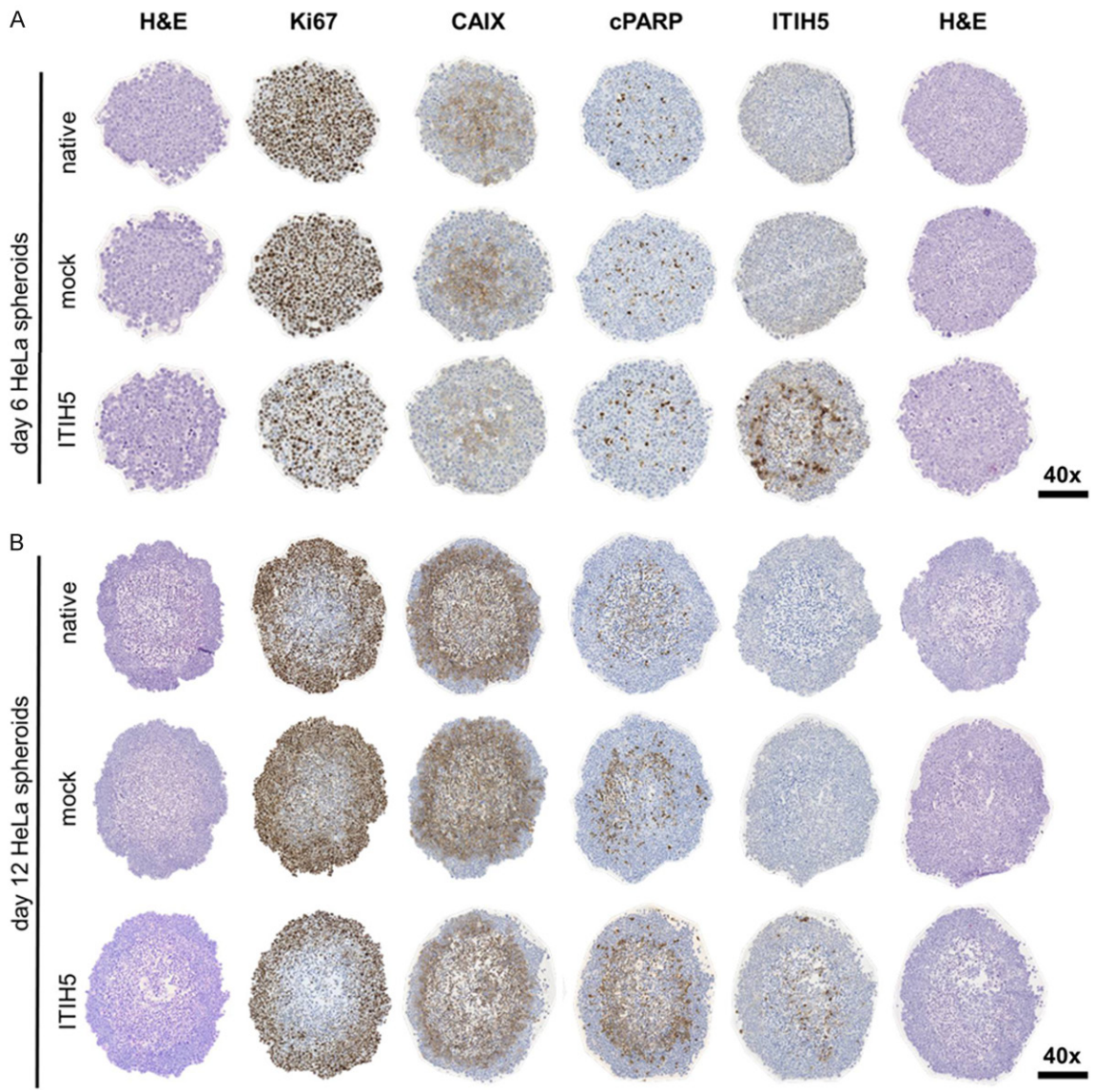

Figure 3. Effect of ITIH5 overexpression on internal structures and different tumorigenic properties of HeLa cells grown as MCTS. (A, B) Representative images of 6-day old (A) and 12-day old (B) FFPE-embedded and sectioned HeLa spheroids, investigated using HE and immunohistochemical staining. Proliferating and apoptotic cells in spheroids derived from native, mock- and ITIH5-transduced HeLa cells were stained with anti-Ki-67 and anti-cPARP, respectively. Hypoxic cells were stained with anti-CAIX. Stable ITIH5 expression was evaluated using anti-ITIH5 antibody. Images represent mid-sections through HeLa cell derived MCTS. Scale bar: 200 µm.

day 12 contained a high proportion of proliferating cells (**Figure 3A**, **3B**) as represented by Ki67 positive nuclei. However, Ki-67-positive staining patterns were not homogenously distributed in spheroids at day 12, and a non-proliferative core could be observed. In ITIH5-overexpressing HeLa spheroids, the number of Ki-67-positive nuclei was clearly diminished (**Figure 4A**). This was further demonstrated by significantly decreased mean percentage levels of proliferating cells in ITIH5 overexpressing HeLa spheroids compared to spheroids derived from native and mock-transduced cells at both time points. A similar distribution pattern of proliferating cells could be observed for SiHa spheroids (Figure S1A, S1B). However, the non-proliferating core was more distinct in spheroids derived from this cell type compared to HeLa spheroids. The highest mean values of Ki-67-positive nuclei were also found in SiHa spheroids on day 6, without significant changes between spheroids derived from native, mock- and ITIH5-transduced cells (**Figure 4B**). In contrast, 12-day old spheroids derived from ITIH5-

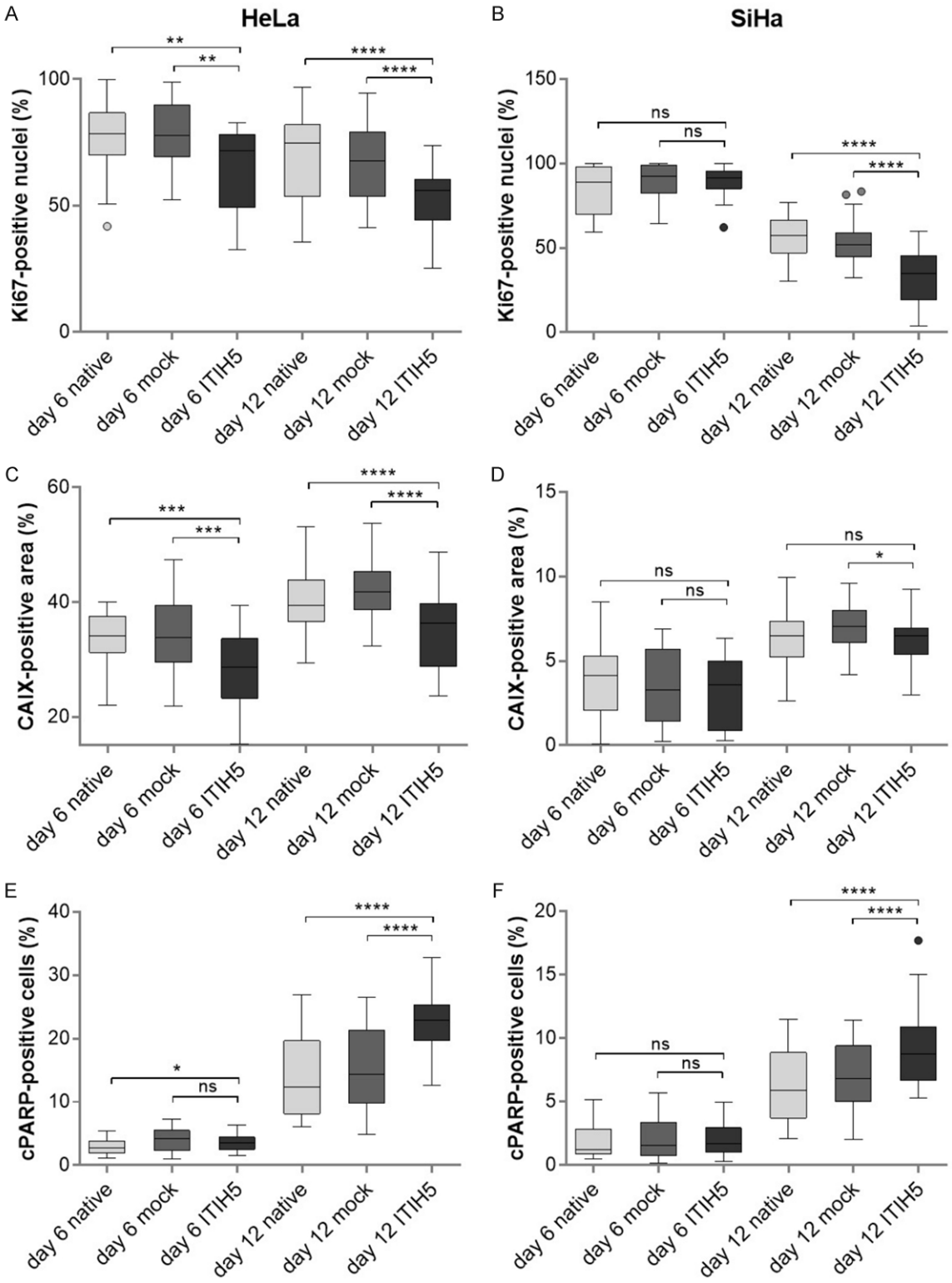

Figure 4. Quantification of ITIH5-induced effects on tumorigenic characteristics in cervical MCTS. FFPE-embedded and sectioned HeLa and SiHa spheroids derived from native, mock- and ITIH5-transduced cells were evaluated on day 6 and day 12 regarding proliferation (Ki67), hypoxia (CAIX) and apoptosis (cPARP). (A, B) The mean ratio of proliferating cells are illustrated as boxplots of Ki67 positive nuclei (%) compared to total nuclei in HeLa (A) and SiHa (B) spheroids. (B, C) The mean ratios of hypoxia within HeLa (C) and SiHa (D) spheroids are displayed as boxplots of CAIX-positive cells (%) compared to total cells. (E, F) Apoptotic cells are presented as boxplots of cPARP-positive

cells (%) compared to total amount of cells in HeLa (E) and SiHa (F) spheroids. In total, 3-4 sections of 8 spheroids at both time points and each sample group were examined (n = 3). Horizontal lines: grouped medians. Boxes: 25-75% quartiles. Vertical lines: range, peak and minimum, ns: not significant $^{*}P < 0.05$, $^{**}P < 0.01$, $^{***}P < 0.001$, $^{****}P < 0.0001$ for the indicated comparisons.

overexpressing SiHa cells exhibited a significant reduction of proliferating cells compared to spheroids of native and mock-transduced cells.

CAIX-positively stained cells, indicating hypoxia [43] and extracellular acidification [44] were mainly located at the inner regions of HeLa spheroids after 6 days, whereas an additional localization of CAIX-positive cells was observable at the spheroid periphery on day 12 (**Figure 3A**, **3B**). Notably, ITIH5-overexpressing spheroids exhibit a reduced CAIX expression, indicated by more faintly stained cells. Quantitative analyses reveal that for both time points, the mean percentages of CAIX-positively stained cells were significantly reduced upon forced ITIH5 expression in HeLa spheroids compared to spheroids derived from native and mock-transduced cells (**Figure 4C**). Endogenous CAIX expression was distinctly lower in SiHa spheroids as compared to HeLa spheroids (**Figure 4C**, **4D**). Interestingly, positively stained cells were mainly located at the spheroid periphery, while almost no staining was detectable in the inner regions of SiHa spheroids (Figure S1A, S1B). The proportion of hypoxic and acidic regions was not significantly different between spheroids derived from native, mock- and ITIH5-transduced SiHa cells on day 6 (**Figure 4D**). At day 12, SiHa spheroids overexpressing ITIH5 showed a significant reduction of CAIX-positive cells compared to spheroids of mock-transduced spheroids; however, no significant difference was detectable between native and ITIH5-overexpressing spheroids.

IHC analysis of cPARP, as a marker for apoptosis, revealed a more pronounced localization of apoptotic cells within the inner region of HeLa spheroids as demonstrated by representative images of stained spheroid sections (**Figure 3A**, **3B**). Moreover, an increase in apoptotic cells could be observed in HeLa spheroids overexpressing ITIH5. This was further highlighted by comparing mean percentages of cPARP-positive cells of day 12 spheroids (**Figure 4E**). The mean of positive cPARP staining in HeLa spheroids overexpressing ITIH5 was significantly increased compared to spheroids derived from native and mock-transduced cells. On day 6, a significant difference in the number of cPARP-positive cells could be obtained between native and ITIH5-overexpressing HeLa spheroids only. SiHa spheroids exhibit a similar pattern of apoptotic cell localization, although with less staining intensities in comparison to HeLa spheroids (Figure S1A, S1B). Nevertheless, a higher rate of cPARP-positive cells was observable for ITIH5-overexpressing SiHa spheroids, when compared to spheroids derived from native and mock-transduced cells. Quantification revealed no difference in mean percentages of cPARP-positively stained cells between spheroids of native, mock- and ITIH5-transduced cells on day 6 (**Figure 4F**). In contrast, a significant increase in apoptotic cells was observable for SiHa spheroids overexpressing ITIH5 on day 12 as compared to spheroids derived from native and mock-transduced cells.

In summary, both spheroid models derived from HeLa and SiHa cells formed densely packed spheroids, with concentric arranged layers comprised of a proliferating rim, followed by a layer of non-proliferating cells and additional areas of cell death within the inner region. ITIH5 overexpression could be successfully detected in the corresponding spheroids after MCTS formation but did not alter spheroid morphology. Ki-67-positive cells were significantly decreased upon forced ITIH5 expression in both HeLa and SiHa spheroids. A highly significant reduction of CAIX-positive cells in ITIH5-overexpressing spheroids could be observed for HeLa spheroids, while the amount of apoptotic cells was significantly higher in MCTS derived from both HeLa and SiHa cells overexpressing ITIH5.

The susceptibility to cytostatic drugs was not influenced by ITIH5 expression levels

Next, the possibility of increased anti-cancer drug susceptibility by ITIH5 expression was analyzed using the Live/Dead Cytotoxicity Kit. For this purpose, the cell viability within HeLa and SiHa spheroids was investigated after challenging with cisplatin and paclitaxel, two approved cytostatic drugs [40]. Representative

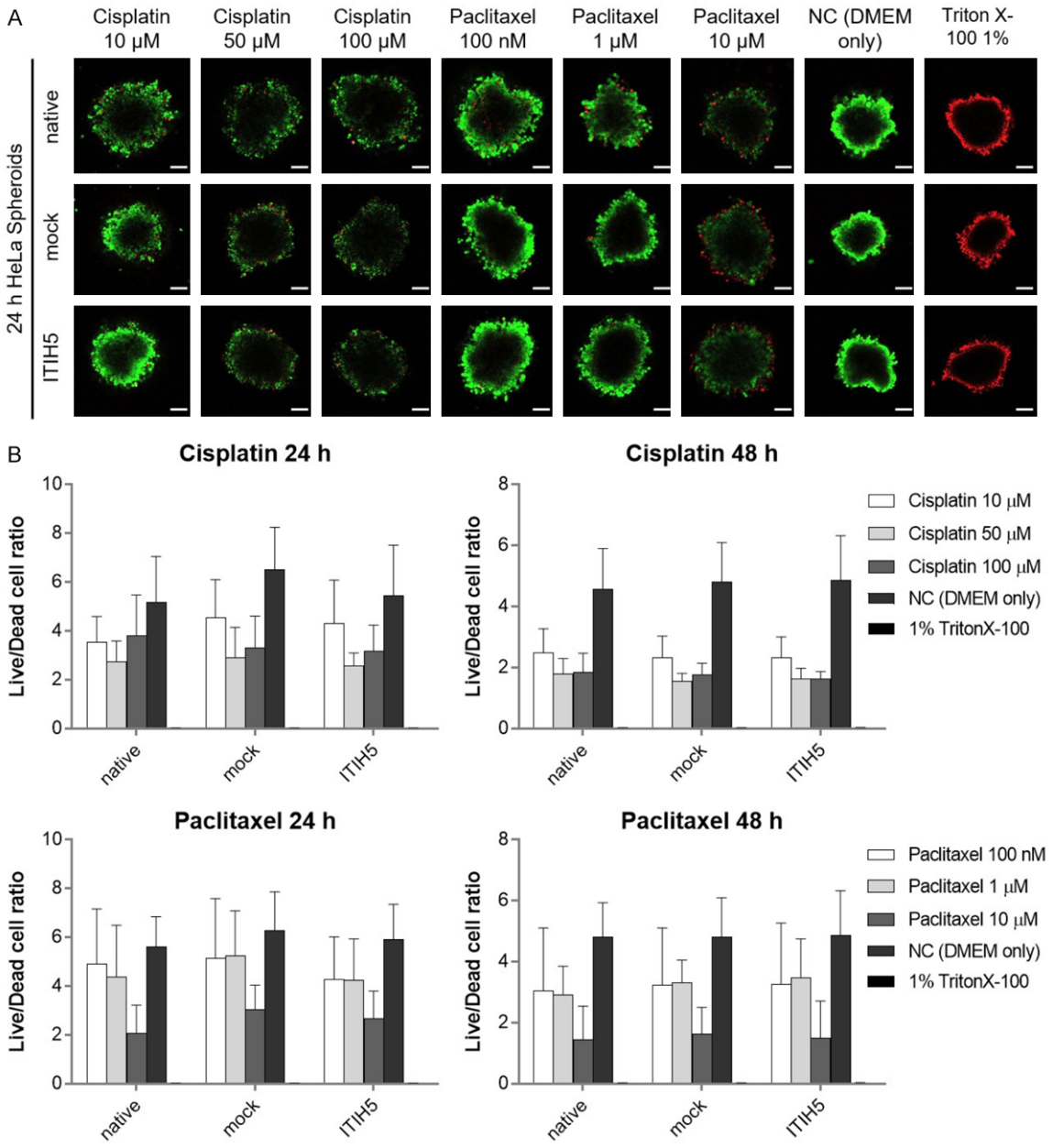

Figure 5. Live/Dead-Assay of MCTS derived from HeLa cells upon cytostatic drug treatment. Drug sensitivity of 8-days old tumor spheroids derived from native, mock- and ITIH5-transduced HeLa cells was investigated upon treatment with cisplatin and paclitaxel for 24 and 48 h, respectively. Incubation with medium only served as negative control and treatment with 1% Triton X-100 as positive control. A. Representative images of 24 h-treated HeLa spheroids. Staining was performed using the Live/Dead Cytotoxicity Kit followed by cLSM. Green fluorescent cells characterize viable cells, while dead cells appear in red. B. Live/Dead cell ratios were calculated based on mean grey values of the corresponding fluorescence intensities. Bars represent mean ± SD of 4 spheroids per condition (n = 3). Scale bar: 100 µm.

images of HeLa (**Figure 5A**) and SiHa (Figure S2A) spheroids obtained 24 h after treatment with cisplatin and paclitaxel, illustrated an overall decrease of viable cells (green fluorescent signal) and an increase of dead cells (red fluorescent signal) with increasing drug concentrations. The reduction of viable cells was further demonstrated by calculating Live/Dead cell ratios, which decreased in a time-dependent manner and with increasing drug concen-

trations for both HeLa (**Figure 5B**) and SiHa (Figure S2B) spheroids. However, Live/Dead cell ratios of HeLa and SiHa spheroids derived from native and mock-transduced cells did not differ from ITIH5 overexpressing spheroids upon treatment with cisplatin or paclitaxel, respectively, suggesting no direct influence of forced ITIH5 expression on cytostatic drug susceptibility of HeLa and SiHa spheroids.

Discussion

Apart from persistent infections with hrHPV as the main causative agent for CC [6], additional (epi)genetic host cell alterations are compulsory for driving malignancy [9, 10]. The elucidation of such molecular mechanisms and their functional impact could be of diagnostic and prognostic value in the clinic. The present study therefore aimed to gain insights into the functional relevance of ITIH5, a potential TSG in CC, in 3D cell culture systems derived from two cervical cancer cell lines (HeLa and SiHa).

The established cervical tumor spheroids derived from transduced HeLa and SiHa cells were employed to further explore the functional impact of forced ITIH5 expression on different tumorigenic characteristics. At first, we demonstrated a clear growth-retardation of spheroids derived from HeLa and SiHa cells upon ITIH5 re-expression in a time-dependent manner. This finding corresponds well to outcomes of other studies, where a growth suppressive effect of ITIH5 was described for several cancer cell lines [13, 22, 27]. However, these latter results were derived from analyses with conventional 2D cell culture models and no studies are yet available on the effects of ITIH5 in an *in vitro* 3D setting.

Tumor cell invasion is a fundamental step in the process of tumorigenesis and is considerably influenced by the ECM [42]. Therefore, Matrigel™-embedded tumor spheroids were employed to elucidate the functional impact of ITIH5 re-expression on tumor cell invasiveness. In line with ITIH5-mediated suppression of tumor spheroid growth, forced ITIH5 expression in HeLa and SiHa spheroids significantly reduced the invasive phenotype. Of note, the observed effect was more striking for SiHa spheroids, indicating a cell line-specific effect upon ITIH5 overexpression. In contrast to the results of the present study, a previous report did not observe less invasive capabilities of cervical cancer cell lines upon ITIH5 expression [13]. However, these latter experiments were performed with transwell-invasion assays, lacking the spatial geometry of tumor cells and their surrounding matrix. Migratory cells can substantially differ in their morphology and mode of migration depending on whether they are moving on 2D or 3D substrates [45]. Other research groups have also found differences between 2D and 3D cancer cell cultures, especially in terms of the impact of extracellular matrix (ECM) [46, 47]. In a 3D ECM-based model, breast cancer cells showed a significantly reduced proliferation rate in comparison to cell culture in 2D conditions after treatment with doxorubicin [48]. The doxorubicin resistance in this breast cancer cells was mediated by extracellular matrix proteins, which were only built in 3D model [48]. This underscores the relevance of 3D *in vitro* models, which are superior to 2D culture models when simulating reorganization of ECM and invasive properties [49]. In line with our findings in cervical cancer cells, another report revealed inhibition of abrogated invasive growth patterns in a 3D Matrigel™ invasion assay when ITIH5 was overexpressed in MDA-MD-231 breast cancer cells [30]. The signaling cascades by which ITIH5 suppresses invasion are still not fully understood. According to the study of Rose and colleagues [30], suppression of tumor cell invasion might be explained by ITIH5-mediated modulation of members of the TGF-β superfamily, which are known to influence important signaling cascades involved in invasion and metastasis [50]. Whether TGF-β-dependent signaling also plays a role in modulating cervical cancer cell invasion remains to be elucidated.

IHC analysis and additional HE-staining of FFPE-embedded HeLa and SiHa spheroid sections revealed a clear distribution in zones of the spheroids at day 12 post-initiation, representing one of the prominent features of tumor spheroids [51]. SiHa spheroids featured a more pronounced area of innermost cell death in comparison to HeLa spheroids. HeLa cells lack αVβ3-integrin expression on their cell surface and therefore establish less cellular interactions with the surrounding ECM compared to SiHa cells [52]. Accordingly, enhanced cell-matrix interactions of SiHa cells might lead to a more densely packed spheroid morphology,

which in turn can increase diffusion limitations and subsequently the amount of central necrosis [51, 53]. No differences in histological features were observed between spheroids derived from native, mock- and ITIH5-transduced HeLa or SiHa cells, respectively. Thus, the impact of ITIH5 on (sub)cellular properties might only be observable on single cell level by applying high-resolution cLSM as performed in another study [29].

A verification of ITIH5 protein expression in tumor spheroids could be successfully confirmed using an immunohistochemical approach. A striking observation is the inhomogeneous distribution of ITIH5 staining throughout spheroids derived from HeLa cells on day 12, with a more pronounced localization within the core regions. Interestingly, the effect was not detectable for 6-days old HeLa spheroids. Stable transgene expression is often provided by CMV promoters [54], as in the case of the ITIH5 expression construct. However, a susceptibility of the CMV promoter to CpG methylation depending on the transcriptional status of the target cell has been reported [55, 56]. Cells within tumor spheroids might become quiescent due to limited nutrient supply, while cells located at the spheroid periphery are still actively proliferating and possess an increased transcriptional level. According to that, it is hypothesized that ITIH5 transiency in peripheral cells of MCTS is correlated to methylation of the promoter sequence.

Spheroid sections were further stained with antibodies directed against Ki-67, CAIX and cPARP, respectively. Overall, Ki-67 expression was mainly localized at the spheroid periphery in HeLa and SiHa spheroids, which is in line with published data about the stratified composition of different cell layers within MCTS [51]. In spheroids derived from both cell types, a significant decrease in Ki-67 positive nuclei could be demonstrated upon ITIH5 re-expression. In the clinic, a high proliferation index as indicated by Ki-67 staining is often positively associated with high grade cervical lesion and a higher risk of progression [57]. Hence, spheroids derived from ITIH5-overexpressing HeLa and SiHa cells feature a lower risk of progression with regard to their decreased Ki-67 staining pattern. This further supports the assumption of ITIH5 to be a novel tumor suppressor in CC.

Furthermore, HeLa spheroids exhibited high ectopic CAIX expression mainly at the core region, which was significantly lower under influence of ITIH5. Aside from representing a general marker for hypoxia and acidosis, CAIX serves as a diagnostic marker in CC and is associated with increased malignancy and a poor clinical outcome [43, 58]. The decreased ectopic CAIX expression in ITH5-overexpressing HeLa spheroids thus underscores the ability of ITIH5 to suppress a tumorigenic phenotype. Although CAIX was primarily expressed at spheroid core regions, an additional localization at the spheroid periphery was especially observed in native and mock-transduced HeLa spheroids on day 12. CAIX appears to be functionally involved in tumor progression [44, 59]. A re-distribution of CAIX to migratory edges and focal contacts is therefore argued to actively contribute to increased migration and invasion [60]. The observed phenomenon might explain the presence of CAIX-positively stained HeLa cells in the corresponding spheroid periphery. A similar re-distribution of CAIX-staining patterns to the spheroid margins on day 6 versus day 12 could be also observed for SiHa spheroids. In contrast, SiHa spheroids overexpressing ITIH5, featured no or only a weak decrease in CAIX-positive area compared to native and mock-transduced spheroids, respectively. In addition, CAIX expression was distinctively lower in comparison to HeLa spheroids, thereby suggesting a strong cell-type dependence of CAIX expression levels.

For evaluating the influence of ITIH5 on the rate of apoptotic cell death, FFPE-embedded spheroid sections were stained with cPARP. IHC analysis revealed positive cPARP staining in the central region of HeLa and SiHa spheroids, which is in line with the described concentric arrangement of MCTS [51]. At day 12, a remarkable increase in cPARP-positive cells could be demonstrated for both, HeLa and SiHa spheroids, overexpressing ITIH5. Accordingly, it can be hypothesized that ITIH5 re-expression leads to an enhanced sensitization to apoptotic signals in the corresponding spheroids. This interpretation is corroborated by corresponding findings as obtained in ITIH5-overexpressing breast cancer cell lines [29]. Until now, nothing is known about underlying mechanisms of ITIH5-arbitrated apoptosis. However, according to a recent study, ITIH5 is responsible for demethylating the promoter region of the well-

characterized tumor suppressor gene DAPK1, thereby inducing its re-expression [29]. To prove this hypothesis, we investigated DAPK1 expression and methylation under the influence of ITIH5 in our two cell culture models. Preliminary results showed that in ITIH5-overexpressed SiHa cells, DAPK1 was more highly expressed, concomitant with decreased DAPK1 methylation in comparison to native and mock-transduced cells (data not shown). For HeLa cells, only marginal increased levels of DAPK1 RNA were observed in ITIH5 overexpressing cells. Moreover, in native HeLa cells, DAPK1 was largely unmethylated. Thus, for HeLa cells, this regulatory mechanism is unlikely. DAPK1 is known to be a positive regulator of apoptotic cell death [61] and is postulated as a downstream effector of ITIH5-mediated tumor suppressive effects [29]. Furthermore, DAPK1 was shown to disrupt matrix survival signals by an inside-out signaling mechanism, thereby impairing β1 integrin-induced suppression of the p53-apoptosis pathway [62]. Thus, it will be interesting to assess the role of DAPK1 for the pro-apoptotic effects of ITIH5 in cervical cancer cells in more detail in future studies.

Re-expression of ITIH5 did not result in significant differences in the susceptibility to cisplatin or paclitaxel in HeLa and SiHa spheroids, respectively. Nevertheless, it cannot necessarily be presumed that ITIH5 has no impact on the sensitivity of tumor cells to anti-cancer agents and further analyses are needed to decipher potential influences. Acquisition of viable and dead cells via cLSM resulted furthermore in dark areas of the innermost spheroid regions, which might be based on diffusion qualities of the fluorescent dyes calcein-AM and EthD-1. Furthermore, laser penetration is restricted to approximately 150 µm due to light absorption and scattering by cellular layers [63]. Accordingly, the use of a two-photon laser, allowing a deeper penetration into tissues, could improve assay performance. In addition, other methods for determining the impact of cytostatic drugs on tumor spheroids should be considered in subsequent studies.

Altogether, the inhibitory effect on spheroid growth, invasion and cellular proliferation as well as an increase in apoptosis upon ITIH5 overexpression corroborates the notion that ITIH5 may act as an important TSG in CC. Further insights into the underlying molecular mechanisms are warranted and are to be elucidated in future studies. Finally, this may aid the development of novel early detection systems, improved prediction of an individuals' patient prognosis as well as to accomplish therapeutic strategies to restore ITIH5 expression in CC.

Acknowledgements

The authors thank PD Dr. J. Müller (Institute of Molecular Cell Biology, Friedrich-Schiller-University, Jena, Germany) for providing the lentiviral packaging plasmids. This work was supported in part by the Brigitte and Dr. Konstanze Wegener-Foundation.

Disclosure of conflict of interest

None.

Address correspondence to: Claudia Backsch, Department of Gynecology and Reproductive Medicine, Jena University Hospital, Friedrich-Schiller-University, Am Klinikum 1, Jena 07747, Germany. Tel: +49-3641 9 390891; Fax: +49-3641 9 390892; E-mail: Claudia.Backsch@med.uni-jena.de

References

[1] Bray F, Ferlay J, Soerjomataram I, Siegel RL, Torre LA and Jemal A. Global cancer statistics 2018: GLOBOCAN estimates of incidence and mortality worldwide for 36 cancers in 185 countries. CA Cancer J Clin 2018; 68: 394-424.

[2] Vizcaino AP, Moreno V, Bosch FX, Munoz N, Barros-Dios XM, Borras J and Parkin DM. International trends in incidence of cervical cancer: II. squamous-cell carcinoma. Int J Cancer 2000; 86: 429-435.

[3] Vizcaino AP, Moreno V, Bosch FX, Munoz N, Barros-Dios XM and Parkin DM. International trends in the incidence of cervical cancer: I. adenocarcinoma and adenosquamous cell carcinomas. Int J Cancer 1998; 75: 536-545.

[4] Richart RM. A modified terminology for cervical intraepithelial neoplasia. Obstet Gynecol 1990; 75: 131-133.

[5] Lee KR and Flynn CE. Early invasive adenocarcinoma of the cervix. Cancer 2000; 89: 1048-1055.

[6] Bosch FX, Lorincz A, Munoz N, Meijer CJ and Shah KV. The causal relation between human papillomavirus and cervical cancer. J Clin Pathol 2002; 55: 244-265.

[7] zur Hausen H. Papillomaviruses and cancer: from basic studies to clinical application. Nat Rev Cancer 2002; 2: 342-350.
[8] Duensing S and Munger K. Mechanisms of genomic instability in human cancer: insights from studies with human papillomavirus oncoproteins. Int J Cancer 2004; 109: 157-162.
[9] Steenbergen RD, Snijders PJ, Heideman DA and Meijer CJ. Clinical implications of (epi)genetic changes in HPV-induced cervical precancerous lesions. Nat Rev Cancer 2014; 14: 395-405.
[10] Solinas-Toldo S, Durst M and Lichter P. Specific chromosomal imbalances in human papillomavirus-transfected cells during progression toward immortality. Proc Natl Acad Sci U S A 1997; 94: 3854-3859.
[11] Poignee M, Backsch C, Beer K, Jansen L, Wagenbach N, Stanbridge EJ, Kirchmayr R, Schneider A and Durst M. Evidence for a putative senescence gene locus within the chromosomal region 10p14-p15. Cancer Res 2001; 61: 7118-7121.
[12] Liesenfeld M, Mosig S, Funke H, Jansen L, Runnebaum IB, Durst M and Backsch C. SORBS2 and TLR3 induce premature senescence in primary human fibroblasts and keratinocytes. BMC Cancer 2013; 13: 507.
[13] Dittmann J, Ziegfeld A, Jansen L, Gajda M, Kloten V, Dahl E, Runnebaum IB, Durst M and Backsch C. Gene expression analysis combined with functional genomics approach identifies ITIH5 as tumor suppressor gene in cervical carcinogenesis. Mol Carcinog 2017; 56: 1578-1589.
[14] Salier JP. Inter-alpha-trypsin inhibitor: emergence of a family within the Kunitz-type protease inhibitor superfamily. Trends Biochem Sci 1990; 15: 435-439.
[15] Salier JP, Rouet P, Raguenez G and Daveau M. The inter-alpha-inhibitor family: from structure to regulation. Biochem J 1996; 315: 1-9.
[16] Bost F, Diarra-Mehrpour M and Martin JP. Inter-alpha-trypsin inhibitor proteoglycan family--a group of proteins binding and stabilizing the extracellular matrix. Eur J Biochem 1998; 252: 339-346.
[17] Zhuo L and Kimata K. Structure and function of inter-alpha-trypsin inhibitor heavy chains. Connect Tissue Res 2008; 49: 311-320.
[18] Hamm A, Veeck J, Bektas N, Wild PJ, Hartmann A, Heindrichs U, Kristiansen G, Werbowetski-Ogilvie T, Del Maestro R, Knuechel R and Dahl E. Frequent expression loss of Inter-alpha-trypsin inhibitor heavy chain (ITIH) genes in multiple human solid tumors: a systematic expression analysis. BMC Cancer 2008; 8: 25.
[19] Paris S, Sesboue R, Delpech B, Chauzy C, Thiberville L, Martin JP, Frebourg T and Diarra-Mehrpour M. Inhibition of tumor growth and metastatic spreading by overexpression of inter-alpha-trypsin inhibitor family chains. Int J Cancer 2002; 97: 615-620.
[20] Werbowetski-Ogilvie TE, Agar NY, Waldkircher de Oliveira RM, Faury D, Antel JP, Jabado N and Del Maestro RF. Isolation of a natural inhibitor of human malignant glial cell invasion: inter alpha-trypsin inhibitor heavy chain 2. Cancer Res 2006; 66: 1464-1472.
[21] Himmelfarb M, Klopocki E, Grube S, Staub E, Klaman I, Hinzmann B, Kristiansen G, Rosenthal A, Dürst M and Dahl E. ITIH5, a novel member of the inter-α-trypsin inhibitor heavy chain family is downregulated in breast cancer. Cancer Lett 2004; 204: 69-77.
[22] Veeck J, Chorovicer M, Naami A, Breuer E, Zafrakas M, Bektas N, Durst M, Kristiansen G, Wild PJ, Hartmann A, Knuechel R and Dahl E. The extracellular matrix protein ITIH5 is a novel prognostic marker in invasive node-negative breast cancer and its aberrant expression is caused by promoter hypermethylation. Oncogene 2008; 27: 865-876.
[23] Oing C, Jost E, Dahl E, Wilop S, Brummendorf TH and Galm O. Aberrant DNA hypermethylation of the ITIH5 tumor suppressor gene in acute myeloid leukemia. Clin Epigenetics 2011; 2: 419-423.
[24] Sasaki K, Kurahara H, Young ED, Natsugoe S, Ijichi A, Iwakuma T and Welch DR. Genome-wide in vivo RNAi screen identifies ITIH5 as a metastasis suppressor in pancreatic cancer. Clin Exp Metastasis 2017; 34: 229-239.
[25] Pita JM, Banito A, Cavaco BM and Leite V. Gene expression profiling associated with the progression to poorly differentiated thyroid carcinomas. Br J Cancer 2009; 101: 1782-1791.
[26] Rose M, Gaisa NT, Antony P, Fiedler D, Heidenreich A, Otto W, Denzinger S, Bertz S, Hartmann A, Karl A, Knuchel R and Dahl E. Epigenetic inactivation of ITIH5 promotes bladder cancer progression and predicts early relapse of pT1 high-grade urothelial tumours. Carcinogenesis 2014; 35: 727-736.
[27] Kloten V, Rose M, Kaspar S, von Stillfried S, Knuchel R and Dahl E. Epigenetic inactivation of the novel candidate tumor suppressor gene ITIH5 in colon cancer predicts unfavorable overall survival in the CpG island methylator phenotype. Epigenetics 2014; 9: 1290-1301.
[28] Dotsch MM, Kloten V, Schlensog M, Heide T, Braunschweig T, Veeck J, Petersen I, Knuchel R and Dahl E. Low expression of ITIH5 in adenocarcinoma of the lung is associated with unfavorable patients' outcome. Epigenetics 2015; 10: 903-912.
[29] Rose M, Kloten V, Noetzel E, Gola L, Ehling J, Heide T, Meurer SK, Gaiko-Shcherbak A, Sechi

AS, Huth S, Weiskirchen R, Klaas O, Antonopoulos W, Lin Q, Wagner W, Veeck J, Gremse F, Steitz J, Knuchel R and Dahl E. ITIH5 mediates epigenetic reprogramming of breast cancer cells. Mol Cancer 2017; 16: 44.

[30] Rose M, Meurer SK, Kloten V, Weiskirchen R, Denecke B, Antonopoulos W, Deckert M, Knuchel R and Dahl E. ITIH5 induces a shift in TGF-beta superfamily signaling involving Endoglin and reduces risk for breast cancer metastasis and tumor death. Mol Carcinog 2018; 57: 167-181.

[31] Yamada KM and Cukierman E. Modeling tissue morphogenesis and cancer in 3D. Cell 2007; 130: 601-610.

[32] Pampaloni F, Reynaud EG and Stelzer EH. The third dimension bridges the gap between cell culture and live tissue. Nat Rev Mol Cell Biol 2007; 8: 839-845.

[33] Pfaffl MW. A new mathematical model for relative quantification in real-time RT-PCR. Nucleic Acids Res 2001; 29: e45.

[34] Ruijter JM, Ramakers C, Hoogaars WM, Karlen Y, Bakker O, van den Hoff MJ and Moorman AF. Amplification efficiency: linking baseline and bias in the analysis of quantitative PCR data. Nucleic Acids Res 2009; 37: e45.

[35] Korff T. Three-dimensional spheroid culture of endothelial cells. Methods in Endothelial Cell Biology 2012; 55.

[36] Foty R. A simple hanging drop cell culture protocol for generation of 3D spheroids. J Vis Exp 2011; 2720.

[37] Schneider CA, Rasband WS and Eliceiri KW. NIH image to ImageJ: 25 years of image analysis. Nat Methods 2012; 9: 671-675.

[38] Vinci M, Box C and Eccles SA. Three-dimensional (3D) tumor spheroid invasion assay. J Vis Exp 2015; e52686.

[39] Ivanov DP and Grabowska AM. Spheroid arrays for high-throughput single-cell analysis of spatial patterns and biomarker expression in 3D. Sci Rep 2017; 7: 41160.

[40] Koh WJ, Greer BE, Abu-Rustum NR, Apte SM, Campos SM, Cho KR, Chu C, Cohn D, Crispens MA, Dorigo O, Eifel PJ, Fisher CM, Frederick P, Gaffney DK, Han E, Huh WK, Lurain JR 3rd, Mutch D, Fader AN, Remmenga SW, Reynolds RK, Teng N, Tillmanns T, Valea FA, Yashar CM, McMillian NR and Scavone JL. Cervical Cancer, Version 2.2015. J Natl Compr Canc Netw 2015; 13: 395-404; quiz 404.

[41] Hanahan D and Weinberg RA. Hallmarks of cancer: the next generation. Cell 2011; 144: 646-674.

[42] Friedl P and Alexander S. Cancer invasion and the microenvironment: plasticity and reciprocity. Cell 2011; 147: 992-1009.

[43] Loncaster JA, Harris AL, Davidson SE, Logue JP, Hunter RD, Wycoff CC, Pastorek J, Ratcliffe PJ, Stratford IJ and West CM. Carbonic anhydrase (CA IX) expression, a potential new intrinsic marker of hypoxia: correlations with tumor oxygen measurements and prognosis in locally advanced carcinoma of the cervix. Cancer Res 2001; 61: 6394-6399.

[44] Ivanov S, Liao SY, Ivanova A, Danilkovitch-Miagkova A, Tarasova N, Weirich G, Merrill MJ, Proescholdt MA, Oldfield EH, Lee J, Zavada J, Waheed A, Sly W, Lerman MI and Stanbridge EJ. Expression of hypoxia-inducible cell-surface transmembrane carbonic anhydrases in human cancer. Am J Pathol 2001; 158: 905-919.

[45] Geraldo S, Simon A and Vignjevic DM. Revealing the cytoskeletal organization of invasive cancer cells in 3D. J Vis Exp 2013; e50763.

[46] Luca AC, Mersch S, Deenen R, Schmidt S, Messner I, Schafer KL, Baldus SE, Huckenbeck W, Piekorz RP, Knoefel WT, Krieg A and Stoecklein NH. Impact of the 3D microenvironment on phenotype, gene expression, and EGFR inhibition of colorectal cancer cell lines. PLoS One 2013; 8: e59689.

[47] Fallica B, Maffei JS, Villa S, Makin G and Zaman M. Alteration of cellular behavior and response to PI3K pathway inhibition by culture in 3D collagen gels. PLoS One 2012; 7: e48024.

[48] Lovitt CJ, Shelper TB and Avery VM. Doxorubicin resistance in breast cancer cells is mediated by extracellular matrix proteins. BMC Cancer 2018; 18: 41.

[49] Kramer N, Walzl A, Unger C, Rosner M, Krupitza G, Hengstschlager M and Dolznig H. In vitro cell migration and invasion assays. Mutat Res 2013; 752: 10-24.

[50] Padua D and Massague J. Roles of TGFbeta in metastasis. Cell Res 2009; 19: 89-102.

[51] Friedrich J, Ebner R and Kunz-Schughart LA. Experimental anti-tumor therapy in 3-D: spheroids--old hat or new challenge? Int J Radiat Biol 2007; 83: 849-871.

[52] Chatterjee N and Chatterjee A. Role of alphavbeta3 integrin receptor in the invasive potential of human cervical cancer (SiHa) cells. J Environ Pathol Toxicol Oncol 2001; 20: 211-221.

[53] Hirschhaeuser F, Menne H, Dittfeld C, West J, Mueller-Klieser W and Kunz-Schughart LA. Multicellular tumor spheroids: an underestimated tool is catching up again. J Biotechnol 2010; 148: 3-15.

[54] Powell SK, Rivera-Soto R and Gray SJ. Viral expression cassette elements to enhance transgene target specificity and expression in gene therapy. Discov Med 2015; 19: 49-57.

[55] Brooks AR, Harkins RN, Wang P, Qian HS, Liu P and Rubanyi GM. Transcriptional silencing is associated with extensive methylation of the CMV promoter following adenoviral gene delivery to muscle. J Gene Med 2004; 6: 395-404.

[56] Hsu CC, Li HP, Hung YH, Leu YW, Wu WH, Wang FS, Lee KD, Chang PJ, Wu CS, Lu YJ, Huang TH, Chang YS and Hsiao SH. Targeted methylation of CMV and E1A viral promoters. Biochem Biophys Res Commun 2010; 402: 228-234.

[57] Kim TH, Han JH, Shin E, Noh JH, Kim HS and Song YS. Clinical implication of p16, Ki-67, and proliferating cell nuclear antigen expression in cervical neoplasia: improvement of diagnostic accuracy for high-grade squamous intraepithelial lesion and prediction of resection margin involvement on conization specimen. J Cancer Prev 2015; 20: 70-77.

[58] Woelber L, Kress K, Kersten JF, Choschzick M, Kilic E, Herwig U, Lindner C, Schwarz J, Jaenicke F, Mahner S, Milde-Langosch K, Mueller V and Ihnen M. Carbonic anhydrase IX in tumor tissue and sera of patients with primary cervical cancer. BMC Cancer 2011; 11: 12.

[59] Shin HJ, Rho SB, Jung DC, Han IO, Oh ES and Kim JY. Carbonic anhydrase IX (CA9) modulates tumor-associated cell migration and invasion. J Cell Sci 2011; 124: 1077-1087.

[60] Svastova E, Witarski W, Csaderova L, Kosik I, Skvarkova L, Hulikova A, Zatovicova M, Barathova M, Kopacek J, Pastorek J and Pastorekova S. Carbonic anhydrase IX interacts with bicarbonate transporters in lamellipodia and increases cell migration via its catalytic domain. J Biol Chem 2012; 287: 3392-3402.

[61] Singh P, Ravanan P and Talwar P. Death associated protein kinase 1 (DAPK1): a regulator of apoptosis and autophagy. Front Mol Neurosci 2016; 9: 46.

[62] Wang WJ, Kuo JC, Yao CC and Chen RH. DAP-kinase induces apoptosis by suppressing integrin activity and disrupting matrix survival signals. J Cell Biol 2002; 159: 169-179.

[63] Wartenberg M and Acker H. Quantitative recording of vitality patterns in living multicellular spheroids by confocal microscopy. Micron 1995; 26: 395-404.

Table S1. Primer sequences, annealing temperatures (T_a) and product sizes used for quantitative PCR

Primer	Sequence	T_a	Product size [bp]
ITIH5	forward 5'-TCACCGTGTGCTTCAACATT-3'	54 °C	107
	reverse 5'-GGGTGCCCCAATTAACTCTC-3'		
ACTB	forward 5'-GCAGTGATCTCCTTCTGCATC-3'	54 °C	294
	reverse 5'-GGACTTCGAGCAAGAGATGG-3'		

bp: base pairs.

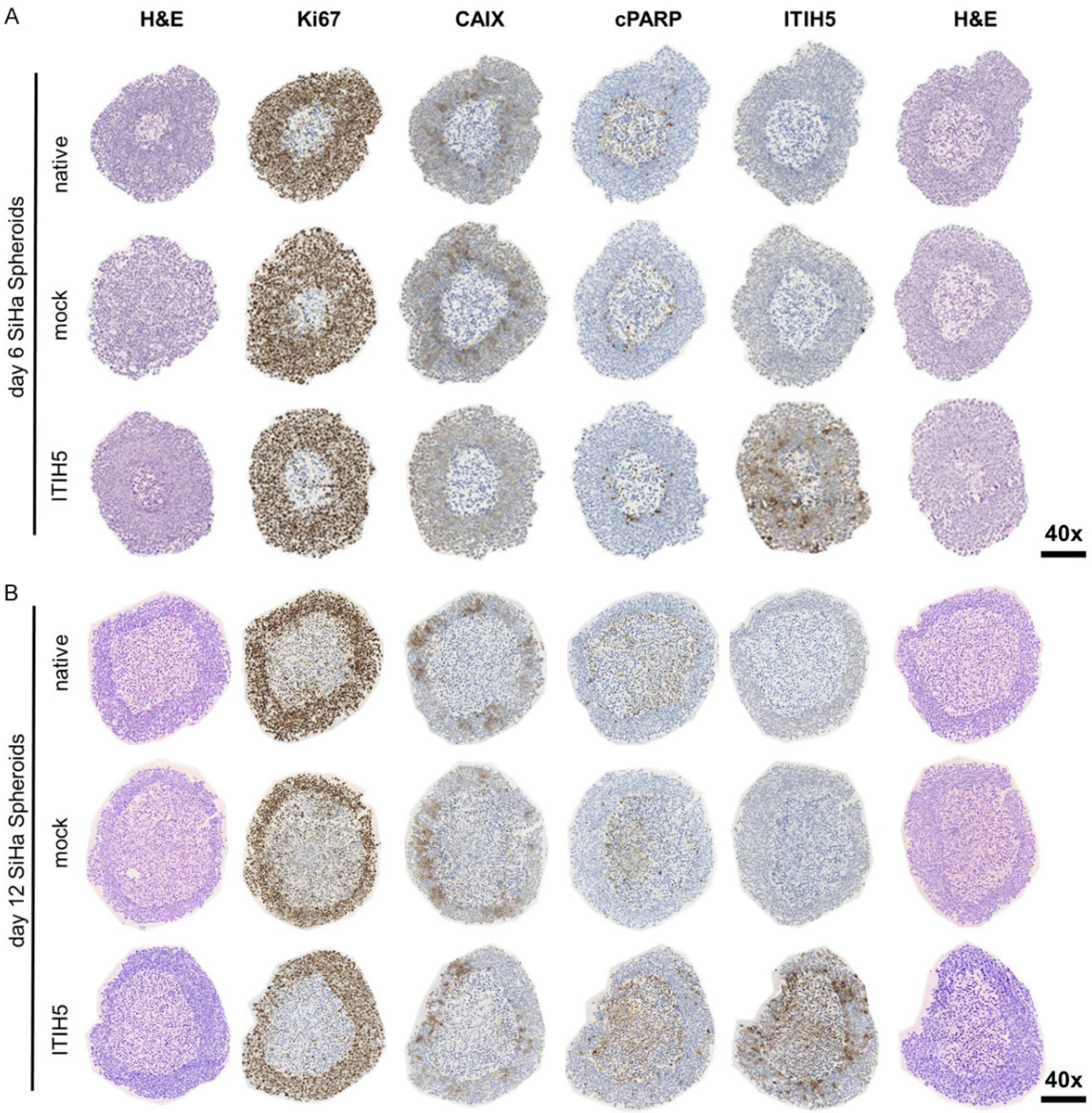

Figure S1. Effect of ITIH5 overexpression on internal structures and different tumorigenic properties of SiHa cells grown MCTS. (A, B) Representative images of 6-day old (A) and 12-day old (B) FFPE-embedded and sectioned SiHa spheroids, investigated using HE and immunohistochemical staining. Proliferating and apoptotic cells in spheroids derived from native, mock- and ITIH5-transduced HeLa cells were stained with Ki-67 and cPARP, respectively. Hypoxic areas were stained with CAIX. Stable ITIH5 expression was evaluated using anti-ITIH5 antibody. Images represent mid-sections through SiHa cell derived MCTS. Scale bar: 200 µm.

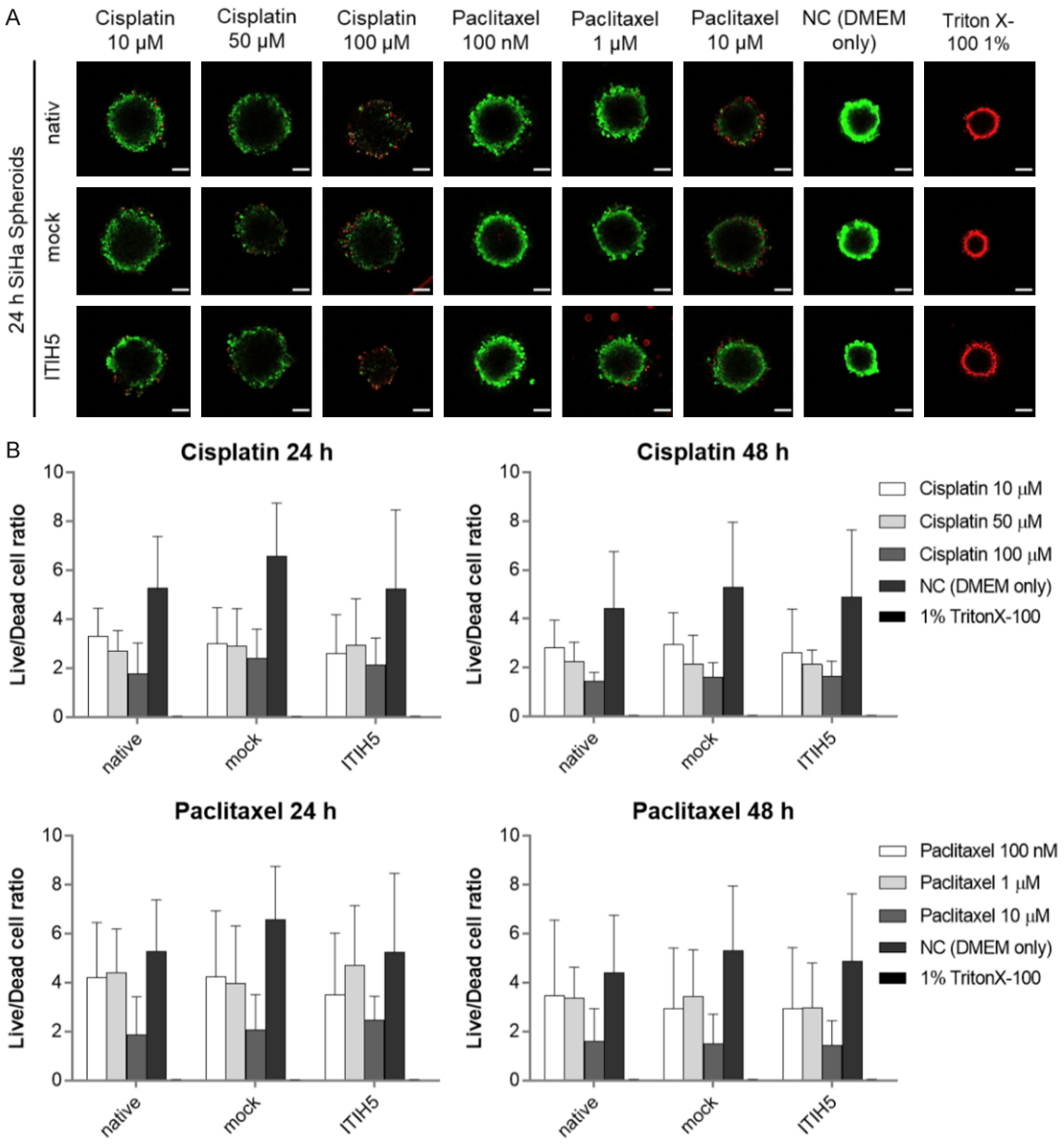

Figure S2. Live/Dead-Assay of MCTS derived from SiHa cells upon cytostatic drug treatment. Drug sensitivity of 8-days old spheroids derived from native, mock- and ITIH5-transduced SiHa cells was investigated under treatment intervention with cisplatin and paclitaxel for 24 and 48 h, respectively (n = 3). Incubation with medium only served as negative control and treatment with 1% Triton X-100 as positive control. A. Representative images of 24 h-treated SiHa spheroids. Staining was performed using the Live/Dead Cytotoxicity Kit followed by cLSM. Green fluorescent cells characterize viable cells, while dead cells appear in red. B. Live/Dead cell ratios were calculated based on mean grey values of the corresponding fluorescence intensities. Bars represent mean ± SD of 4 spheroids per condition. Scale bar: 100 µm.